Published in final edited form as:
Crit Care Med. 2010 February ; 38(2): 612–618. doi:10.1097/CCM.0b013e3181c027ae.

Protective effects of recombinant osteopontin on early brain injury after subarachnoid hemorrhage in rats

Hidenori Suzuki, MD, PhD[1], **Robert Ayer, MD**[2], **Takashi Sugawara, MD, PhD**[1], **Wanqiu Chen, MS**[1], **Takumi Sozen, MD, PhD**[1,*], **Yu Hasegawa, MD, PhD**[1], **Kenji Kanamaru, MD, PhD**[3], and **John H. Zhang, MD, PhD**[1,2]

[1] Department of Physiology, Loma Linda University of Medicine, Loma Linda, USA

[2] Department of Neurosurgery, Loma Linda University of Medicine, Loma Linda, USA

[3] Department of Neurosurgery, Suzuka Kaisei Hospital, Suzuka, Japan

Abstract

Objective—Accumulated evidence suggests that the primary cause of poor outcome after subarachnoid hemorrhage (SAH) is not only cerebral arterial narrowing, but also early brain injury (EBI). Our objective was to determine the effect of recombinant osteopontin (r-OPN), a pleiotropic extracellular matrix glycoprotein, on post-SAH EBI in rats.

Design—Controlled *in vivo* laboratory study.

Setting—Animal research laboratory.

Subjects—One hundred seventy-seven male adult Sprague-Dawley rats, 300–370g.

Interventions—The endovascular perforation model of SAH was produced. SAH or sham-operated rats were treated with an equal volume (1μL) of pre-SAH intracerebroventricular administration of two dosages (0.02 and 0.1μg) of r-OPN, albumin or vehicle. Body weight, neurological scores, brain edema and blood-brain barrier (BBB) disruption were evaluated, and Western blot analyses were performed to determine the effect of r-OPN on matrix metalloproteinase (MMP)-9, substrates of MMP-9 (zona occludens [ZO]-1, laminin), tissue inhibitor of MMP (TIMP)-1, inflammation (interleukin-1β), and nuclear factor (NF)-κ B signaling pathways.

Measurements and Main Results—Treatment with r-OPN prevented a significant loss in body weight, neurological impairment, brain edema, and BBB disruption after SAH. These effects were associated with the deactivation of NF-κB activity, inhibition of MMP-9 induction, the maintenance of TIMP-1, and the consequent preservation of the cerebral microvessel basal lamina protein laminin, and the tight junction protein ZO-1.

Conclusions—These results demonstrate that r-OPN treatment is effective for post-SAH EBI.

Keywords

osteopontin; blood-brain barrier; brain injury; edema; neurological dysfunction; subarachnoid hemorrhage

Address correspondence to: John H. Zhang, MD, PhD. Department of Physiology, Loma Linda University School of Medicine, Risley Hall, Room 223, Loma Linda, CA 92354. johnzhang3910@yahoo.com, Phone: +1-909-558-4000, extension 44723, Fax: +1-909-558-0119.

The work is attributed to: Department of Physiology, Loma Linda University School of Medicine, Loma Linda, CA 92354.

The authors have no potential conflicts of interest to disclose.

Aneurysmal subarachnoid hemorrhage (SAH) is a common and devastating neurological disorder (1). Cerebral vasospasm has been believed to be a leading cause of mortality and morbidity (2). Recent randomized clinical trials, however, showed that clazosentan significantly reduced angiographic vasospasm but failed to improve long-term neurological outcome (3,4). This means that the treatment efforts targeting only angiographic vasospasm might not be enough to achieve a better outcome. Thus, new research efforts have focused on clarifying the pathophysiology of early brain injury (EBI) following SAH, and on developing protective strategies against it (5).

Osteopontin (OPN) is a secreted extracellular matrix (ECM) glycoprotein that is involved in both physiological and pathological processes in a wide range of tissue (6). The biological functions of OPN are highly variable, and often seemingly contradictory depending on the biological scenario surrounding its induction (7). However, there is compelling evidence that OPN can, in a variety of situations, help cells survive an otherwise lethal insult (8). For example, endogenous OPN induction has consistently been found to have protective effects on ischemic injuries involving the brain and other organs (9,10). Moreover, the administration of recombinant OPN (r-OPN) markedly reduced the infarct size via anti-apoptotic actions in a transient focal cerebral ischemia model of mice (11). To date, however, no experimental studies have investigated the effect of r-OPN on EBI or blood-brain barrier (BBB) disruption after SAH. Here, we report a beneficial effect of r-OPN treatment on post-SAH EBI.

MATERIALS AND METHODS

All protocols were approved by the Institutional Animal Care and Use Committee of Loma Linda University. The animals were cared for in accordance with the Guidelines of the Committee.

Experimental Model of SAH and Study Protocol

The endovascular perforation model of SAH was produced in male adult Sprague-Dawley rats (300–370g, Harlan, Indianapolis, IN) as previously described with slight modifications (12–14). Briefly, rats were anesthetized with 3% isoflurane in 60/40% medical air/oxygen in a small animal anesthesia induction box, followed by the subcutaneous injection of atropine (0.1mg/kg). The animals were transorally intubated and the respiration was maintained with a small rodent respirator (Harvard Apparatus, Holliston, MA). Anesthesia was maintained with 2 to 3% isoflurane in 60/40% medical air/oxygen. Blood pressure and blood gas were measured via the left femoral artery. Rectal temperature was kept at approximately 37°C with an electric heating pad. After exposing the left common carotid artery, external carotid artery (ECA) and internal carotid artery (ICA), the ECA was ligated, cut, and shaped into a 3-mm stump. A sharpened 4-0 monofilament nylon suture was advanced rostrally into the ICA from the ECA stump until resistance was felt (15–18mm from the common carotid bifurcation) and then pushed 3mm further to perforate the bifurcation of the anterior and middle cerebral arteries. Immediately after puncture, the suture was withdrawn into the ECA stump, and the ICA was reperfused to produce SAH. Sham-operated rats underwent the identical procedures except that the suture was withdrawn once resistance was felt, without puncture. The incision was then closed, and rats were housed individually following their recovery from anesthesia. Animals had free access to food and water until euthanization.

One hundred seventy-seven rats were randomly divided into 6 groups: sham-operated rats treated with vehicle (n=23) or 0.1μg of r-OPN (n=17), and SAH rats treated with vehicle (n=45), 0.1μg of bovine serum albumin (BSA; n=11), 0.02μg (n=39) or 0.1μg (n=42) of r-OPN. Neurological scores and body weight were evaluated prior to and after the SAH production or sham-operation at each interval of 24 hours until the sacrifice. At the sacrifice, high-resolution pictures of the base of the brain depicting the circle of Willis and basilar arteries

were taken for assessing the severity of SAH under ice cooling. The brain water content measurements and Western blot analyses were performed at 24 hours and BBB permeability was determined at both 24 and 72 hours post-surgery.

Neurological Scoring

Neurological scores were blindly evaluated as previously described (13). The evaluation consists of six tests that can be scored 0–3 or 1–3. These six tests include: spontaneous activity; symmetry in the movement of all four limbs; forepaw outstretching; climbing; body proprioception; and response to whisker stimulation. The maximum score is 18 and the minimum score is 3. Higher scores indicate greater function.

Severity of SAH

The severity of SAH was blindly assessed using the high-resolution photographs as previously described (13). The SAH grading system was as follows: the basal cistern was divided into six segments, and each segment was allotted a grade from 0 to 3 depending on the amount of subarachnoid blood clot in the segment; grade 0: no subarachnoid blood; grade 1: minimal subarachnoid blood; grade 2: moderate blood clot with recognizable arteries; grade 3: blood clot obliterating all arteries within the segment. The animals received a total score ranging from 0 to 18 after adding the scores from all six segments.

Intracerebroventricular Infusion

Rats were placed in a head holder under 2–3% isoflurane anesthesia. The needle of a 10-μL Hamilton syringe (Microliter #701; Hamilton Company, Reno, NV) was inserted through a burr hole perforated on the skull into the left lateral ventricle using the following coordinates relative to bregma: 1.5mm posterior; 1.0mm lateral; 3.2mm below the horizontal plane of bregma (15). Sterile saline vehicle (1μL), BSA (0.1μg in 1μL; EMD Chemicals, La Jolla, CA) or mouse r-OPN (0.02 or 0.1μg in 1μL; EMD Chemicals, La Jolla, CA) was automatically infused at a rate of 0.1μL/minute irrespective of the animal's body weight at one hour before the SAH production or sham-operation. The needle was removed 10 minutes after finishing of an infusion, and the burr hole was quickly plugged with a bone wax.

Brain Water Content

After sacrificing rats, brains were immediately divided into the right and left cerebral hemispheres, brain-stem and cerebellum, and weighed (wet weight). Brain specimens were dried in an oven at 105°C for 72 hours and weighed again (dry weight). The following formula was used to calculate the percentage of water content: ([wet weight - dry weight]/wet weight) × 100% (16).

BBB Permeability

At 24 or 72 hours post-surgery, Evans blue dye (2%; 5mL/kg) was injected over 2 minutes into the left femoral vein and allowed to circulate for 60 minutes. Under deep anesthesia, rats were sacrificed by intracardial perfusion with phosphate-buffered saline and brains were removed and divided into the same regions as the water content study. Brain specimens were weighed, homogenized in 1mL of phosphate-buffered saline, and centrifuged at 15,000*g* for 30 minutes. Then, 0.6mL of the resultant supernatant was added to an equal volume of trichloroacetic acid. After overnight incubation at 4°C and centrifugation at 15,000*g* at 4°C for 30 minutes, the supernatant was taken for spectrophotometric quantification of extravasated Evans blue dye at 615nm as previously described (16).

Western Blot Analyses

Western blot analysis was performed as previously described (12). Briefly, the whole left (perforation side) cerebral hemispheres were homogenized, and aliquots of each fraction were used to determine the protein concentration of each sample using a detergent compatible assay (Bio-Rad, Hercules, CA). Equal amounts of protein samples (50μg) were loaded on a Tris glycine gel, electrophoresed, and transferred to a nitrocellulose membrane. Membranes were then blocked with a blocking solution, followed by incubation overnight at 4°C with the primary antibodies: mouse monoclonal anti-OPN (1:200), rabbit polyclonal anti-inhibitor of nuclear factor (NF)-kB (IκB)-α (1:200), goat polyclonal anti-phospho-IκB-α (1:200), goat polyclonal anti-phospho-IκB kinase (IKK) α/β (1:200) antibodies (Santa Cruz Biotechnology, Santa Cruz, CA), goat polyclonal anti-human interleukin (IL)-1β antibody (1:500, BioVision Research Products, Mountain View, CA), rabbit polyclonal anti-zona occludens (ZO)-1 antibody (1:200, Invitrogen Corporation, Carlsbad, CA), rabbit polyclonal anti-matrix metalloproteinase (MMP)-9 (1:1500), mouse monoclonal anti-tissue inhibitor of MMP (TIMP)-1 (1:1000) antibodies (Millipore Biosciences Research Reagents SBU, Temecula, CA), and mouse monoclonal anti-laminin antibody (1:200, EMD Chemicals, La Jolla, CA). Immunoblots were processed with appropriate secondary antibodies (1:2000, Santa Cruz Biotechnology, Santa Cruz, CA) for 1 hour at 21°C, and bands were detected with a chemiluminescence reagent kit (ECL Plus; Amersham Bioscience, Arlington Heights, IL). Blot bands were quantified by densitometry with Image J software (Image J 1.40g, NIH). β-Actin (1:2000, Santa Cruz Biotechnology, Santa Cruz, CA) was blotted on the same membrane as a loading control.

Statistics

Neurological scores were expressed as median±25th–75th percentiles, and were analyzed using Kruskal-Wallis test, followed by Steel-Dwass multiple comparisons. Other values were expressed as mean±SD, and chi-square test and repeated-measures analysis of variance with Scheffe correction were used as appropriate. Stepwise linear regression evaluated independent predictors of Evans blue dye extravasation at 72 hours post-SAH. The $p<0.05$ was considered significant.

RESULTS

Exogenous OPN Prevents Post-SAH BBB Disruption

Comparisons of physiological parameters revealed no significant differences among the groups (data not shown). None of the sham-operated rats died within the 72-hour observation period. In SAH rats, the mortality in 0.1μg of r-OPN treatment group (11.9%, 5 of 42 rats) tended to be lower but was not significantly different from the other groups (17.8% [8 of 45 rats], 18.2% [2 of 11 rats] and 17.9% [7 of 39 rats] in vehicle, BSA, and 0.02μg of r-OPN treatment groups, respectively). The average SAH grading score was 10.8±4.1 at 24 hours (n=88) and 7.6±4.8 at 72 hours (n=27) post-SAH. Since the severity of brain injuries in the endovascular perforation model of SAH is correlated with SAH grading scores (13,14), SAH was placed into 2 categories, mild (a total score of 9 or less at 24 hours [n=27], or 6 or less at 72 hours post-SAH [n=9]) and severe (a total score of 10 or more at 24 hours [n=61], or 7 or more at 72 hours post-SAH [n=18]). Vehicle-treated mild SAH rats (n=5) did not significantly increase Evans blue dye extravasation compared with sham-operated rats (n=12) at 24 hours post-SAH (Data not shown). Thus, further analysis was performed on severe SAH rats, in which the vessel rupture was consistently at the bifurcation of the anterior and middle cerebral arteries.

The average SAH grading score in severe SAH rats was similar among the groups in each analysis (12.4±1.9, 12.8±1.2, 13.6±2.5 and 12.3±2.2 in the vehicle, BSA, 0.02 and 0.1μg of r-OPN treatment groups at 24 hours; 9.8±1.7, 11.2±1.2 and 9.7±2.2 in the vehicle, 0.02 and

0.1μg of r-OPN treatment groups at 72 hours post-SAH). This indicates similar injury amongst compared groups, and suggests that differences in outcomes are the result of different treatments.

Pre-SAH administration of 0.1μg of r-OPN significantly prevented a loss in body weight and neurological impairment compared with the vehicle- and BSA-treated SAH groups at 24 and 72 hours post-SAH (Fig. 1). SAH caused a significant increase in Evans blue dye extravasation in all brain regions, which was significantly attenuated by both dosages of r-OPN treatment in the bilateral cerebral hemispheres at 24 hours post-SAH (Fig. 2). As a control, we injected BSA, a protein with an equivalent weight to r-OPN, and excluded the possibility of a non-specific response to intracerebroventricular protein injection. At 72 hours post-SAH, Evans blue dye extravasation in the left cerebral hemisphere and brain-stem was still elevated in vehicle- and BSA-treated SAH rats, and a significant linear correlation was observed between Evans blue dye extravasation in the left cerebral hemisphere and neurological scores ($r=-0.716$, $p<0.005$). In linear regression analysis, however, r-OPN treatment, but not neurological and SAH grading scores, was the only independent factor associated with Evans blue dye extravasation at 72 hours post-SAH (F ratio=20.7, $p<0.005$).

Similarly, post-SAH increases in brain water content were significantly reduced by r-OPN treatment in the bilateral cerebral hemispheres at 24 hours post-SAH (Fig. 3). r-OPN had no effects on body weight loss, neurological impairment, Evans blue dye extravasation and brain water content in sham-operated rats (Fig. 1, 2 and 3).

Exogenous OPN Prevents Post-SAH MMP-9 Induction and TIMP-1 Reduction

Western blot analysis of the left cerebral hemisphere showed that SAH significantly increased active MMP-9 expression and decreased its corresponding inhibitor TIMP-1 expression, which were significantly inhibited by r-OPN treatment at 24 hours post-SAH (Fig. 4, *A* and *B*). Post-SAH degradation of laminin and ZO-1, which are basement membrane and inter-endothelial tight junction proteins of cerebral microvessels, respectively, and substrates of MMP-9, was also significantly suppressed by r-OPN treatment (Fig. 4, *C* and *D*). A significant linear correlation was observed between the active MMP-9 level and the TIMP-1 ($r=-0.914$, $p<0.0001$), laminin ($r=-0.686$, $p<0.005$) and ZO-1 ($r=-0.724$, $p<0.005$) levels.

Exogenous OPN does not Inhibit IL-1β Induction but Suppresses NF-κB Activation After SAH

Cleaved IL-1β levels were significantly elevated in SAH rats compared with sham-operated rats, but r-OPN did not suppress cleaved IL-1β levels (Fig. 5). In vehicle-treated SAH rats, an increased phosphorylation of IKKα/β and IκB-α, along with a degradation of IκB-α, was shown, demonstrating the NF-κB activation (17). This activation was significantly inhibited by r-OPN treatment (Fig. 6), and phosphorylated IκB-α was significantly correlated with active MMP-9 levels ($r=0.864$, $p<0.0001$).

Exogenous OPN Suppresses Endogenous OPN Induction After SAH

SAH caused endogenous OPN induction (Fig. 7). r-OPN treatment did not change endogenous OPN levels in the sham-operated rats, but significantly suppressed endogenous OPN induction after SAH. These findings may reflect the decreased brain damage after r-OPN treatment.

DISCUSSION

In this study, pre-SAH intracerebroventricular administration of r-OPN demonstrated significant prevention against EBI as measured by reductions in post-SAH loss in body weight, neurological impairment, brain edema, and BBB disruption. This protection was provided by

r-OPN-mediated deactivation of NF-κB activity, thereby improving the balance between proteolytic (MMP-9) and matrix stabilizing factors (TIMP-1).

A key pathologic manifestation of post-SAH EBI is an increase in BBB permeability, which leads to vasogenic edema. Global cerebral edema, or BBB dysfunction, has been described as an independent risk factor for poor outcome after SAH (18). BBB dysfunction may allow greater influx of blood-borne cells and substances into brain parenchyma, thus amplifying inflammation, leading to further parenchymal damage and edema formation (19). Post-SAH BBB breakdown, however, is a transient phenomenon and a functional recovery may ensue, although the intrinsic mechanisms to reverse BBB disruption are unknown. OPN is induced in response to tissue injuries or inflammation, and may play a role in the maintenance of tissue homeostasis and the induction of tissue repair in a variety of situations (8–10). Our unpublished data also showed that the blockage of endogenous OPN induction aggravated post-SAH neurological impairment and BBB disruption. These findings suggest that OPN may represent a naturally occurring protective factor against EBI after SAH, supporting the results in this study.

Accumulated evidence supports a role for MMP-9 in the early BBB disruption of neuroinflammatory diseases or stroke (20,21). MMP-9 degrades the ECM of cerebral microvessel basal lamina, including collagen IV, laminin, fibronectin, and inter-endothelial tight junction proteins such as ZO-1, causing BBB disruption after SAH (16,21). A balanced interaction between MMP-9 and TIMP-1 may determine the severity of BBB disruption and neuronal apoptosis after insults (22). The activation of NF-κB has been detected in the cerebral cortices adjacent to SAH (19), and is known to directly regulate the transcription of MMP-9 and TIMP-1 in addition to orchestrating the inflammatory cascade (23,24).

OPN regulates the bioavailability of MMPs, although the effects exerted by OPN on MMPs differ depending on cell types, receptor interactions, post-translational modifications, and the phosphorylation state of OPN (7,25,26). For example, OPN alone has no effect on MMP-9 activity or expression, nor does it affect NF-κB activity in various non-tumor culture cells (27–29), while on the other hand, OPN increased MMP-9 activity in human newborn aortic smooth muscle cells in the presence of platelet-derived growth factor-BB, as well as in many tumor cells (26,28). There are also several studies demonstrating OPN's role as an inhibitor of MMP-9 and NF-κB activity, such as OPN's inhibition of IL-1β-stimulated increases in activities and expression of MMP-9 in adult rat cardiac fibroblasts (29), and OPN's prevention of NF-κB activation and nitric oxide synthesis in IL-1β and endotoxin treated non-tumor cells (27,30). Our data also demonstrate OPN's role as an inhibitor of MMP-9 and NF-κB activity in the presence of proinflammatory cytokines, in our case IL-1β elevation following SAH. Given these data we hypothesize that the inhibitory effects of OPN on MMP-9 and NF-κB activities may be observed only in the presence of proinflammatory cytokines.

IL-1β has been repeatedly reported to be induced in the brain after SAH and cause brain injuries (31,32). IL-1β-induced MMP-9 secretion from astrocytes is critically dependant on NF-κB signaling pathways (33), and the direct inhibition of NF-κB prevented IL-1β-stimulated increases in MMP-9 expression and activity in adult rat cardiac fibroblasts (17). Our study demonstrates similar effects in an *in vivo* model. However, our study showed that OPN's inactivation of NF-κB had no effect on IL-1β levels. Previous experiments using OPN knockout mice showed increased IL-1β gene expression in ischemic brain injury (10), while others have shown that reducing NF-κB activity reduced IL-1β levels after myocardial infarction (24). Our diverging findings may be explained by IL-1β induction via NF-κB-independent mechanisms, such as post-SAH sympathetic activation or catecholamine release (34,35). On the other hand, oxidative stress also up-regulates MMP-9 levels in brain (20). Since the oxidative stress-

dependent MMP-9 induction is accompanied by NF-κB activation (36), OPN might inactivate NF-κB by reducing oxidative stress (6,9). In this regard, further studies are needed.

This study had some limitations. First, rats were anesthetized with isoflurane, which has been shown to have neuroprotection (37). Thus, a combined effect of r-OPN and isoflurane cannot be excluded. Secondly, r-OPN was given via an intracerebroventricular injection as a pre-treatment. This diminishes the translational significance of the study, and the effects of post-treatment and other administration methods should be examined before clinical trials. Thirdly, we did not examine the effect of r-OPN on vasospasm or cerebral blood flow that might contribute to neurological improvement, although OPN has not been reported to affect vessel diameters. Considering pleiotropic effects of OPN, it would be worth examining if OPN has protective effects on post-SAH pathology other than the BBB protection observed in this study.

In conclusion, we demonstrate for the first time that r-OPN treatment prevented EBI or BBB disruption after SAH. r-OPN treatment is promising, and our findings warrant more research.

Acknowledgments

This study was partially supported by grants (NS053407) from the National Institutes of Health to J.H.Z.

References

1. Suarez JI, Tarr RW, Selman WR. Aneurysmal subarachnoid hemorrhage. N Engl J Med 2006;354:387–396. [PubMed: 16436770]
2. Bederson JB, Connolly ES Jr, Batjer HH, et al. Guidelines for the management of aneurysmal subarachnoid hemorrhage: a statement for healthcare professionals from a special writing group of the Stroke Council, American Heart Association. Stroke 2009;40:994–1025. [PubMed: 19164800]
3. Vajkoczy P, Meyer B, Weidauer S, et al. Clazosentan (AXV-034343), a selective endothelin A receptor antagonist, in the prevention of cerebral vasospasm following severe aneurysmal subarachnoid hemorrhage: results of a randomized, double-blind, placebo-controlled, multicenter phase IIa study. J Neurosurg 2005;103:9–17. [PubMed: 16121967]
4. Macdonald RL, Kassell NF, Mayer S, et al. Clazosentan to overcome neurological ischemia and infarction occurring after subarachnoid hemorrhage (CONSCIOUS-1). Randomized, double-blind, placebo-controlled phase 2 dose-finding trial. Stroke 2008;39:3015–3021. [PubMed: 18688013]
5. Cahill J, Calvert JW, Zhang JH. Mechanisms of early brain injury after subarachnoid hemorrhage. J Cereb Blood Flow Metab 2006;26:1341–1353. [PubMed: 16482081]
6. Mazzali M, Kipari T, Ophascharoensuk V, et al. Osteopontin. A molecule for all seasons. Q J Med 2002;95:3–13.
7. Kazanecki CC, Uzwiak DJ, Denhardt DT. Control of osteopontin signaling and function by post-translational phosphorylation and protein folding. J Cell Biochem 2007;102:912–924. [PubMed: 17910028]
8. Denhardt DT, Noda M, O'Regan AW, et al. Osteopontin as a means to cope with environmental insults: regulation of inflammation, tissue remodeling, and cell survival. J Clin Invest 2001;107:1055–1061. [PubMed: 11342566]
9. Xie Y, Sakatsume M, Nishi S, et al. Expression, roles, receptors, and regulation of osteopontin in the kidney. Kidney Int 2001;60:1645–1657. [PubMed: 11703581]
10. Schroeter M, Zickler P, Denhardt DT, et al. Increased thalamic neurodegeneration following ischaemic cortical stroke in osteopontin-deficient mice. Brain 2006;129:1426–1437. [PubMed: 16636021]
11. Meller R, Stevens SL, Minami M, et al. Neuroprotection by osteopontin in stroke. J Cereb Blood Flow Metab 2005;25:217–225. [PubMed: 15678124]
12. Kusaka G, Ishikawa M, Nanda A, et al. Signaling pathways for early brain injury after subarachnoid hemorrhage. J Cereb Blood Flow Metab 2004;24:916–925. [PubMed: 15362722]

13. Sugawara T, Ayer R, Jadhav V, et al. A new grading system evaluating bleeding scale in filament perforation subarachnoid hemorrhage rat model. J Neurosci Methods 2008;167:327–334. [PubMed: 17870179]

14. Ayer RE, Sugawara T, Chen W, et al. Melatonin decreases mortality following severe subarachnoid hemorrhage. J Pineal Res 2008;44:197–204. [PubMed: 18289172]

15. Allen RM, Uban KA, Atwood EM, et al. Continuous intracerebroventricular infusion of the competitive NMDA receptor antagonist, LY235959, facilitates escalation of cocaine self-administration and increases break point for cocaine in Sprague-Dawley rats. Pharmacol Biochem Be 2007;88:82–88.

16. Yatsushige H, Ostrowski RP, Tsubokawa T, et al. Role of c-Jun N-terminal kinase in early brain injury after subarachnoid hemorrhage. J Neurosci Res 2007;85:1436–1448. [PubMed: 17410600]

17. Xie Z, Singh M, Singh K. Differential regulation of matrix metalloproteinase-2 and -9 expression and activity in adult rat cardiac fibroblasts in response to interleukin-1β. J Biol Chem 2004;279:39513–39519. [PubMed: 15269222]

18. Claassen J, Carhuapoma JR, Kreiter KT, et al. Global cerebral edema after subarachnoid hemorrhage: Frequency, predictors, and impact on outcome. Stroke 2002;33:1225–1232. [PubMed: 11988595]

19. Simard JM, Geng Z, Woo SK, et al. Glibenclamide reduces inflammation, vasogenic edema, and caspase-3 activation after subarachnoid hemorrhage. J Cereb Blood Flow Metab 2009;29:317–330. [PubMed: 18854840]

20. Petty MA, Lo EH. Junctional complexes of the blood-brain barrier: permeability changes in neuroinflammation. Prog Neurobiol 2000;68:311–323. [PubMed: 12531232]

21. Sehba FA, Mostafa G, Knopman J, et al. Acute alterations in microvascular basal lamina after subarachnoid hemorrhage. J Neurosurg 2004;101:633–640. [PubMed: 15481718]

22. Fujimoto M, Takagi Y, Aoki T, et al. Tissue inhibitor of metalloproteinases protect blood-brain barrier disruption in focal cerebral ischemia. J Cereb Blood Flow Metab 2008;28:1674–1685. [PubMed: 18560439]

23. Bond M, Chase AJ, Baker AH, et al. Inhibition of transcription factor NF-κB reduces matrix metalloproteinase-1, -3 and -9 production by vascular smooth muscle cells. Cardiovasc Res 2001;50:556–565. [PubMed: 11376631]

24. Trescher K, Bernecker O, Fellner B, et al. Inflammation and postinfarct remodeling: Overexpression of IκB prevents ventricular dilation via increasing TIMP levels. Cardiovasc Res 2006;69:746–754. [PubMed: 16388787]

25. Weber GF, Zawaideh S, Hikita S, et al. Phosphorylation-dependent interaction of osteopontin with receptors regulates macrophage migration and activation. J Leukoc Biol 2002;72:752–761. [PubMed: 12377945]

26. Rangaswami H, Bulbule A, Kundu GC. Osteopontin: Role in cell signaling and cancer progression. Trends Cell Biol 2006;16:79–87. [PubMed: 16406521]

27. Arafat HA, Katakam AK, Chipitsyna G, et al. Osteopontin protects the islets and β-cells from interleukin-1β-mediated cytotoxicity through negative feedback regulation of nitric oxide. Endocrinology 2007;148:575–584. [PubMed: 17110428]

28. Bendeck MP, Irvin C, Reidy M, et al. Smooth muscle cell matrix metalloproteinase production is stimulated via alpha(v)beta(3) integrin. Arterioscler Thromb Vasc Biol 2000;20:1467–1472. [PubMed: 10845859]

29. Xie Z, Singh M, Siwik DA, et al. Osteopontin inhibits interleukin-1β-stimulated increases in matrix metalloproteinase activity in adult rat cardiac fibroblasts: Role of protein kinase C-ζ. J Biol Chem 2003;278:48546–48552. [PubMed: 14500723]

30. Guo H, Cai CQ, Schroeder RA, et al. Osteopontin is a negative feedback regulator of nitric oxide synthesis in murine macrophages. J Immunol 2001;166:1079–1086. [PubMed: 11145688]

31. Holmin S, Mathiesen T. Intracerebral administration of interleukin-1beta and induction of inflammation, apoptosis, and vasogenic edema. J Neurosurg 2000;92:108–120. [PubMed: 10616089]

32. Sugawara T, Jadhav V, Ayer R, et al. Thrombin inhibition by argatroban ameliorates early brain injury and improves neurological outcomes after experimental subarachnoid hemorrhage in rat. Stroke 2009;40:1530–1532. [PubMed: 19228846]

33. Wu CY, Hsieh HL, Jou MJ, et al. Involvement of p42/p44 MAPK, p38 MAPK, JNK and nuclear factor-kappa B in interleukin-1beta-induced matrix metalloproteinase-9 expression in rat brain astrocytes. J Neurochem 2004;90:1477–1488. [PubMed: 15341531]

34. Naredi S, Lambert G, Friberg P, et al. Sympathetic activation and inflammatory response in patients with subarachnoid haemorrhage. Intens Care Med 2006;32:1955–1961.

35. Tan KS, Nackley AG, Satterfield K, et al. β2 adrenergic receptor activation stimulates pro-inflammatory cytokine production in macrophages via PKA- and NF-κB-independent mechanisms. Cell Signal 2007;19:251–260. [PubMed: 16996249]

36. Kolev K, Skopal J, Simon L, et al. Matrix metalloproteinase-9 expression in post-hypoxic human brain capillary endothelial cells: H_2O_2 as a trigger and NF-kappaB as a signal transducer. Thromb Haemost 2003;90:528–537. [PubMed: 12958623]

37. Matchett GA, Allard MW, Martin RD, et al. Neuroprotective effect of volatile anesthetic agents: Molecular mechanisms. Neurol Res 2009;31:128–134. [PubMed: 19298752]

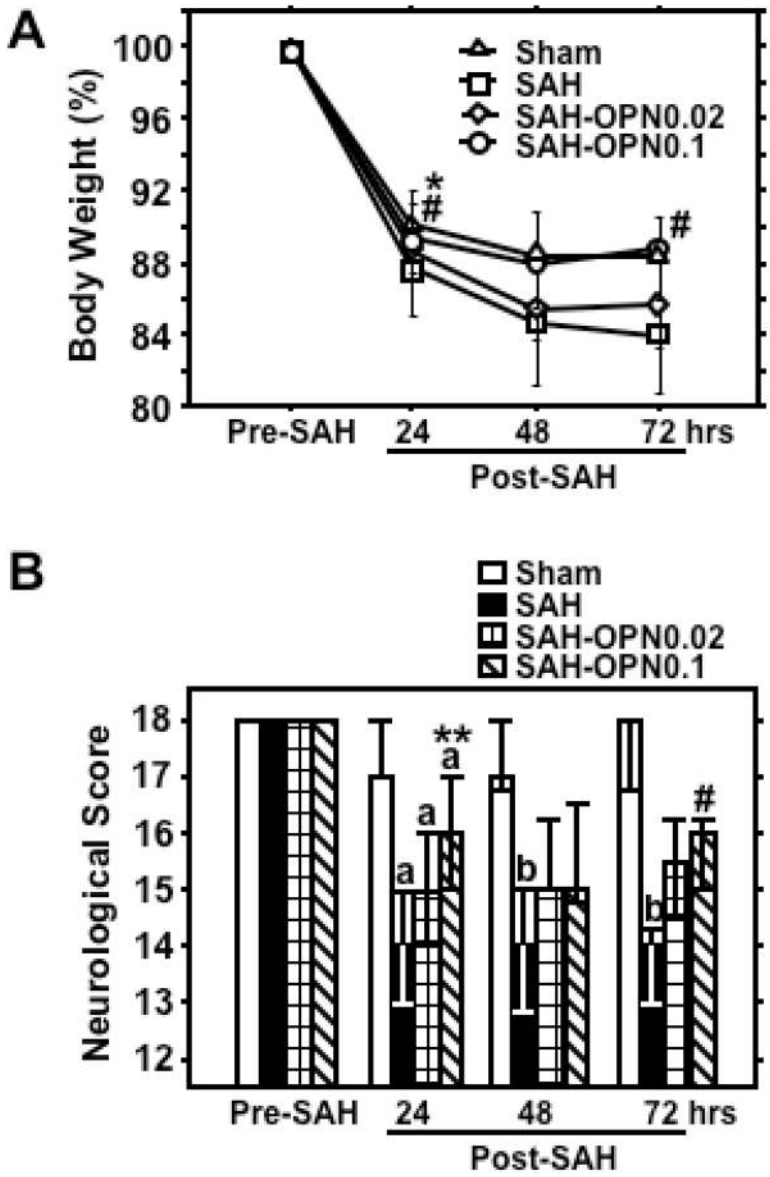

Figure 1.

Effects of recombinant osteopontin (OPN) treatment on body weight (***A***; mean±SD) and neurological score (***B***; median±25th–75th percentiles) after subarachnoid hemorrhage (SAH). *Sham*, Sham-operated rats treated with saline or OPN, n=40 (saline, 23; OPN, 17; pre-SAH, 24 hrs post-SAH) or 6 (saline, 6; 48, 72 hrs post-SAH); *SAH*, SAH rats treated with vehicle or bovine serum albumin (BSA), n=29 (saline, 23; BSA, 6; pre-SAH, 24 hrs post-SAH) or 6 (saline, 6; 48, 72 hrs post-SAH); *SAH-OPN0.02*, SAH rats treated with 0.02μg of OPN, n=23 (pre-SAH, 24 hrs post-SAH) or 6 (48, 72 hrs post-SAH); *SAH-OPN0.1*, SAH rats treated with 0.1μg of OPN, n=23 (pre-SAH, 24 hrs post-SAH) or 6 (48, 72 hrs post-SAH); *p<0.0005, **p<0.01, $^{\#}p$<0.05 vs. SAH group; ^{a}p<0.01, ^{b}p<0.05 vs. sham group.

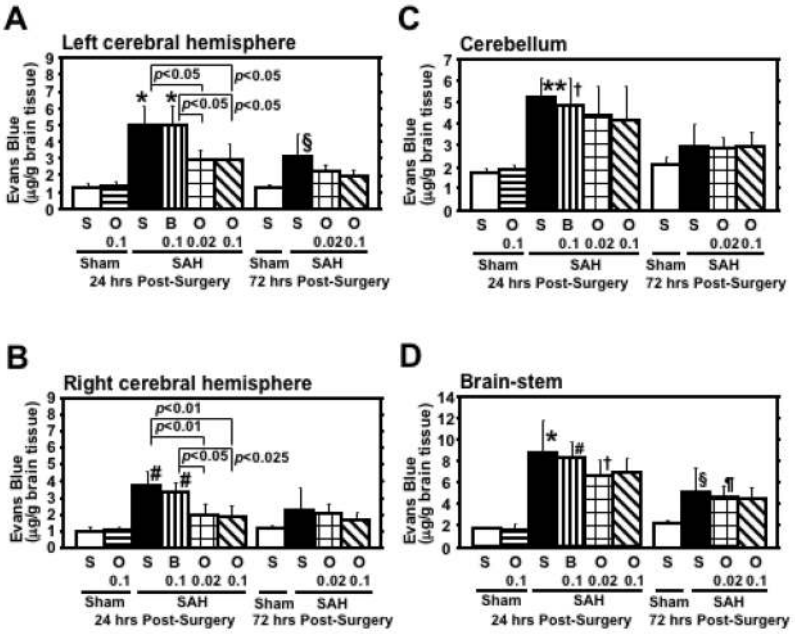

Figure 2.

Effects of recombinant osteopontin (OPN) treatment on Evans blue dye extravasation in the brain after subarachnoid hemorrhage (SAH). B 0.1, O 0.02, O 0.1, S, rats treated with bovine serum albumin (0.1μg), OPN (0.02μg), OPN (0.1μg) or saline, respectively; n=6 rats per group; $^{*}p<0.0001$, $^{\#}p<0.001$, $^{**}p<0.005$, $^{\dagger}p<0.05$ vs. sham-operated rats treated with saline or OPN at 24 hours post-surgery; $^{\S}p<0.025$, $^{\P}p<0.05$ vs. sham-operated rats treated with saline at 72 hours post-surgery; error bar, SD.

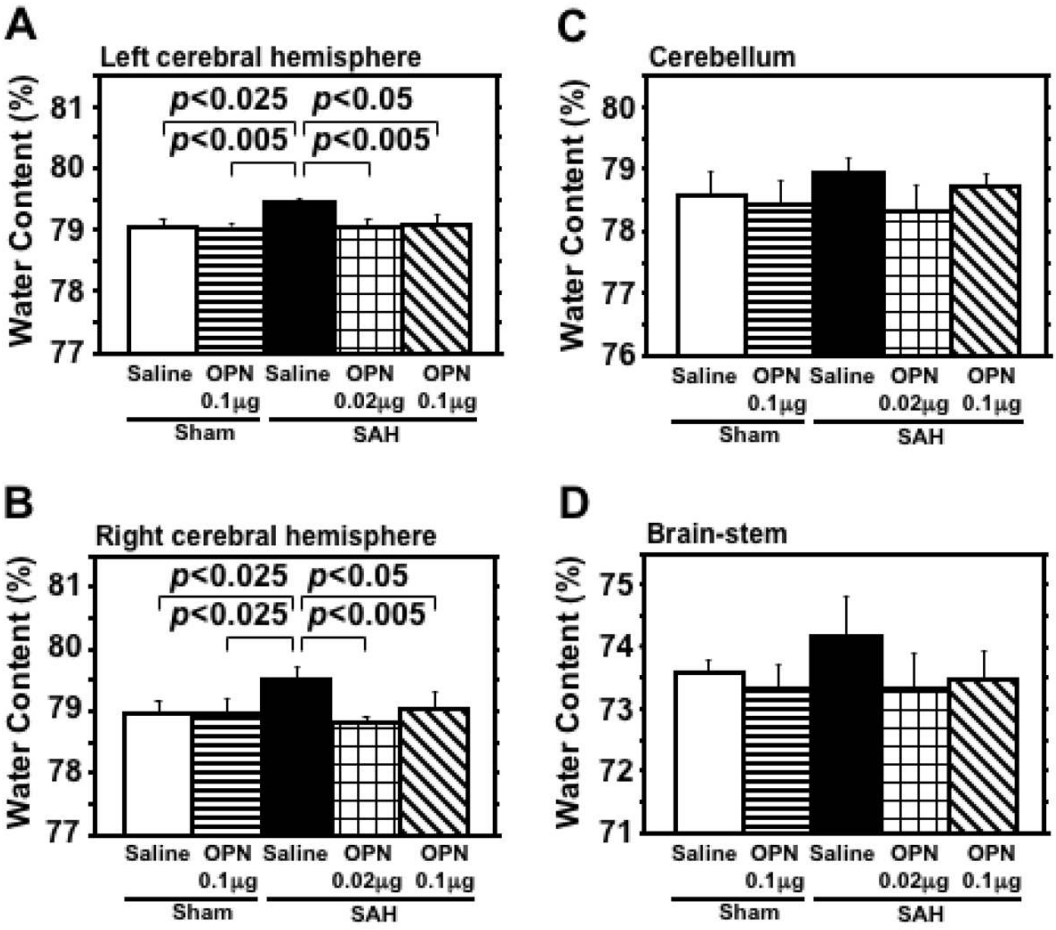

Figure 3.
Effects of recombinant osteopontin (OPN) treatment on brain water content at 24 hours after subarachnoid hemorrhage (SAH). N=5 rats per group; error bar, SD.

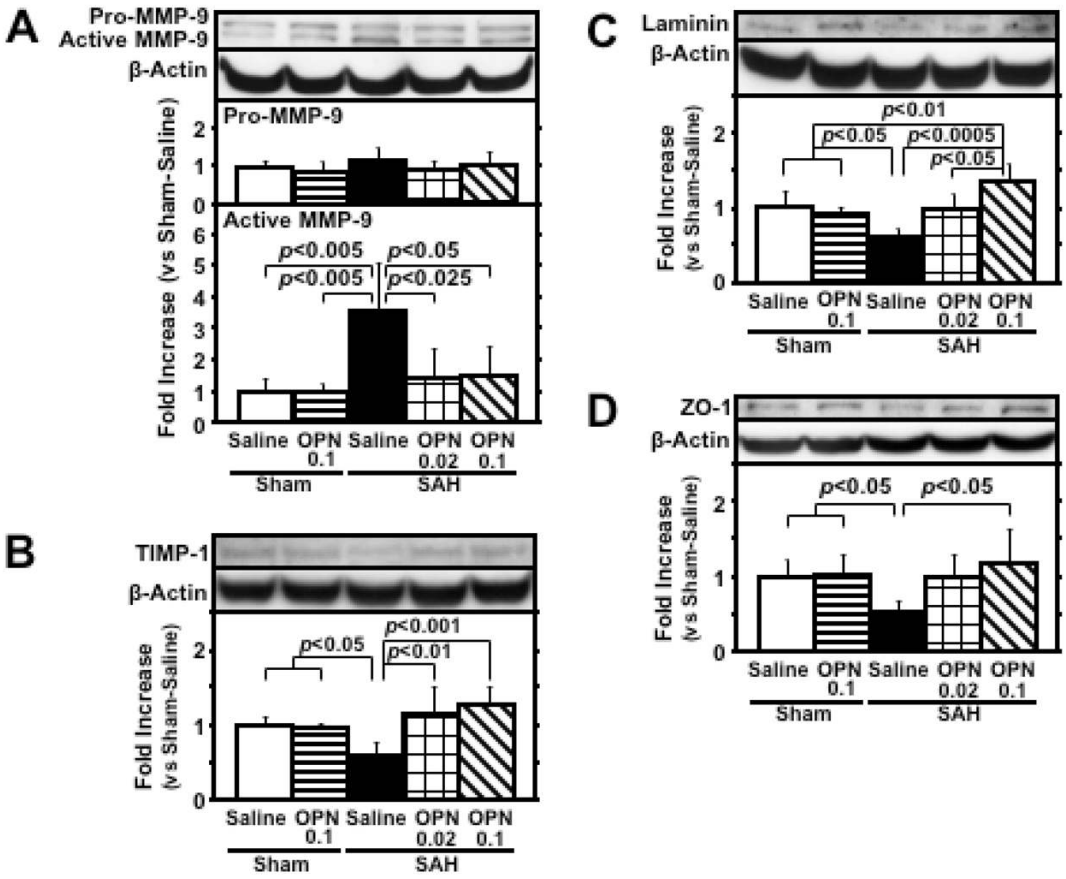

Figure 4.

Effects of recombinant osteopontin (OPN) treatment on matrix metalloproteinase (MMP)-9 induction and tissue inhibitor of MMP (TIMP)-1 reduction in the left cerebral hemisphere at 24 hours after subarachnoid hemorrhage (SAH). Western blots for MMP-9 (***A***), TIMP-1 (***B***), laminin (***C***) and zona occludens (ZO)-1 (***D***). Expression levels of each protein in Western blot are expressed as a ratio of β-actin levels for normalization. N=6 rats per group; error bar, SD.

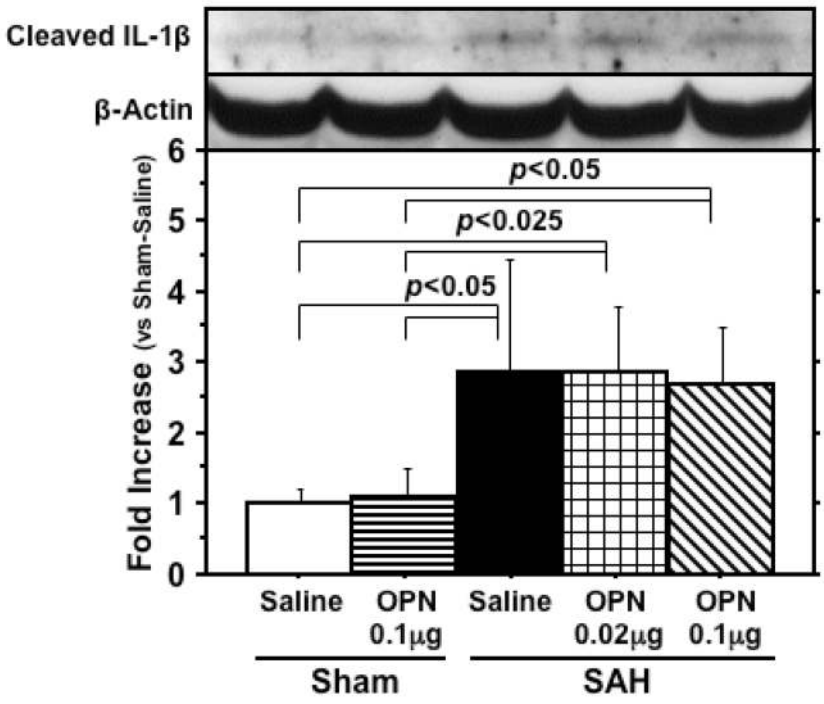

Figure 5.

Western blot for cleaved interleukin (IL)-1β in the left cerebral hemisphere at 24 hours after subarachnoid hemorrhage (SAH). The expression levels are expressed as a ratio of β-actin levels for normalization. N=6 rats per group; error bar, SD.

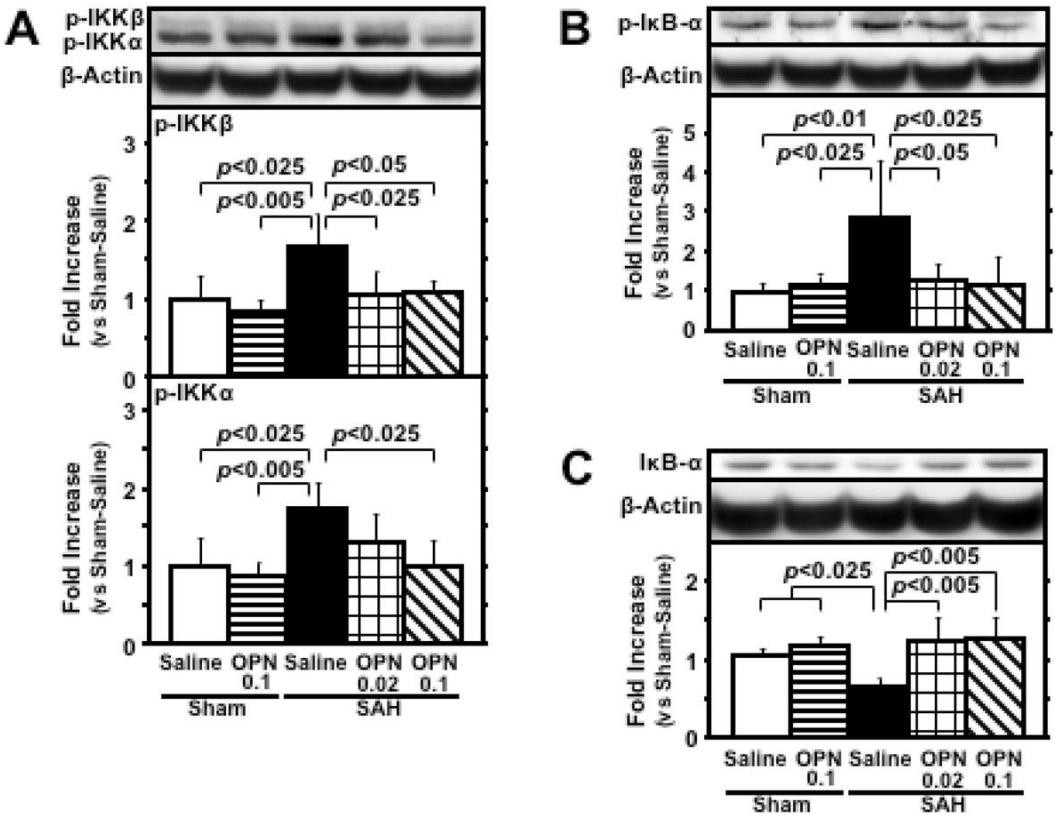

Figure 6.

Effects of recombinant osteopontin (OPN) treatment on nuclear factor (NF)-κB activation in the left cerebral hemisphere at 24 hours after subarachnoid hemorrhage (SAH). Western blots for phosphorylated inhibitor of NF-kB (IκB) kinase (IKK) α/β (p-IKKα/β; ***A***), phosphorylated IκB-α (p-IκB-α; ***B***) and IκB-α (***C***). Expression levels of each protein in Western blot are expressed as a ratio of β-actin levels for normalization. N=6 rats per group; error bar, SD.

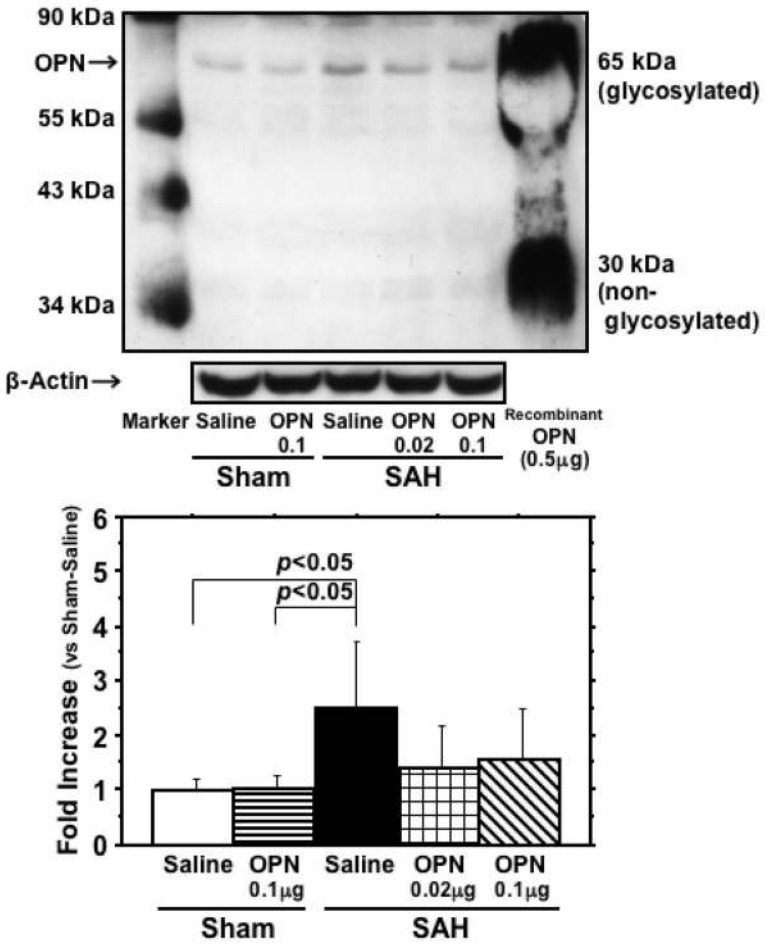

Figure 7.

Effects of recombinant osteopontin (OPN) treatment on endogenous OPN induction in the left cerebral hemisphere at 24 hours after subarachnoid hemorrhage (SAH). The expression levels are expressed as a ratio of β-actin levels for normalization. N=6 rats per group; error bar, SD.